Systems/Circuits

# Correlation between OFF and ON Channels Underlies Dark Target Selectivity in an Insect Visual System

**Steven D. Wiederman,[1] Patrick A. Shoemaker,[2] and David C. O'Carroll[1]**

[1]Adelaide Centre for Neuroscience Research, School of Medical Sciences, The University of Adelaide, Adelaide, SA 5005, Australia, and [2]Tanner Research Inc., Monrovia, California 91016

**In both vertebrates and invertebrates, evidence supports separation of luminance increments and decrements (ON and OFF channels) in early stages of visual processing (Hartline, 1938; Joesch et al., 2010); however, less is known about how these parallel pathways are recombined to encode form and motion. In *Drosophila*, genetic knockdown of inputs to putative ON and OFF pathways and direct recording from downstream neurons in the wide-field motion pathway reveal that local elementary motion detectors exist in pairs that separately correlate contrast polarity channels, ON with ON and OFF with OFF (Joesch et al., 2013). However, behavioral responses to reverse-phi motion of discrete features reveal additional correlations of the opposite signs (Clark et al., 2011). We here present intracellular recordings from feature detecting neurons in the dragonfly that provide direct physiological evidence for the correlation of OFF and ON pathways. These neurons show clear polarity selectivity for feature contrast, responding strongly to targets that are darker than the background and only weakly to dark contrasting edges. These dark target responses are much stronger than the linear combination of responses to ON and OFF edges. We compare these data with output from elementary motion detector-based models (Eichner et al., 2011; Clark et al., 2011), with and without stages of strong center-surround antagonism. Our data support an alternative elementary small target motion detector model, which derives dark target selectivity from the correlation of a delayed OFF with an un-delayed ON signal at each individual visual processing unit (Wiederman et al., 2008, 2009).**

## Introduction

The dominant computational model for biological motion processing for 50 years, the Hassenstein-Reichardt (HR) model for an elementary motion detector (EMD), involves correlation of spatially separated contrast signals after delaying one channel (see Fig. 1*A*). This model is supported by diverse evidence from behavioral and electrophysiological studies, particularly in dipteran flies (Hassenstein and Reichardt, 1956; for review, see Borst and Euler, 2011), but its specific neural implementation remains elusive. In particular, the degree to which contrast signals are separated into parallel ON and OFF pathways (for luminance increments and decrements) and then recombined within the EMD has been questioned for many years (Egelhaaf and Borst, 1985; Franceschini et al., 1989). Data from downstream Vertical and Horizontal System neurons in dipteran flies support a 2-detector EMD (see Fig. 1*B*) in which ON-ON and OFF-OFF information is correlated locally in parallel pathways, which are then summed (Eichner et al., 2011; Joesch et al., 2013).

Although a role for HS and other lobula plate tangential cells in optomotor responses of many insects is beyond doubt, 80% of the neurons in the third optic ganglion lie in a parallel structure, the lobula (Strausfeld, 1976), which could provide alternative pathways using different combinations of OFF and ON signals. Although only a small proportion of these neurons have yet been studied, some respond to different classes of visual motion such as, small features, edges, or looming stimuli (O'Shea and Williams, 1974; O'Carroll, 1993; Nordström and O'Carroll, 2006). One such class, small target motion detector (STMD) neurons, has been characterized in the lobula and lateral midbrain of both dragonflies (O'Carroll, 1993; Geurten et al., 2007) and dipteran flies (Nordström and O'Carroll, 2006; Barnett et al., 2007). Typical STMDs respond robustly to small moving targets (subtending ~1–3°), even against background clutter (Nordström and O'Carroll, 2006; Wiederman and O'Carroll, 2011).

In an attempt to explain these properties, we previously proposed a model for an elementary small target motion detector (ESTMD) using a correlation of ON signals at each location with delayed OFF to match the expected signature of a small, dark feature (see Fig. 1*D*). Despite the ESTMD model providing an excellent fit to the spatiotemporal tuning of STMD neurons, several key predictions of it remain untested. In this paper, we present recordings from several types of dragonfly STMD and present evidence for a potent nonlinear interaction between OFF and ON channels in this alternative motion pathway. We show that many STMD neurons only respond to dark objects, with little or no response to light objects with equal contrast. These responses are greater than predicted from the linear combination of responses to dark or light edges of identical, limited lateral extent. Finally, we show that classical HR-EMD models (either with or without strong surround antagonism) cannot account for our data, but

Received March 25, 2013; revised June 30, 2013; accepted July 9, 2013.

Author contributions: S.D.W., P.A.S., and D.C.O. designed research; S.D.W. performed research; S.D.W., P.A.S., and D.C.O. analyzed data; S.D.W., P.A.S., and D.C.O. wrote the paper.

This work was supported by the Australian Research Council's Discovery Projects funding scheme (project number DP130104572) and the US Air Force Office of Scientific Research (FA2386-10-1-4114, FA9550-09-1-0116). We thank the manager of the Botanic Gardens in Adelaide for allowing insect collection.

The authors declare no competing financial interests.

Correspondence should be addressed to Dr. Steven D. Wiederman, Adelaide Centre for Neuroscience Research, School of Medical Sciences, The University of Adelaide, Adelaide, SA 5005, Australia. E-mail: steven.wiederman@adelaide.edu.au.

DOI:10.1523/JNEUROSCI.1277-13.2013

 0270-6474/13/3313225-08$15.00/0

our model of STMD neurons is well matched (Wiederman et al., 2008, 2010). Thus, we provide evidence that feature-specific information is extracted by operations involving the supralinear combination of ON and OFF contrast pathways in the dragonfly brain.

## Materials and Methods

*Physiological recording.* We inserted aluminum silicate glass microelectrodes (filled with 2 M KCl, 80–120 MΩ) into the brain of immobilized *Hemicordulia tau* ($n = 13$, either sex). We recorded intracellularly from individual neurons, identifying STMDs from their size tuning and characteristic receptive field, mapped using 37 horizontal and 21 vertical scans of a 1.25° dark target across a 120 Hz HD LCD monitor (100° × 80° viewing extent) at 45°/s (for full details of these methods, see Bolzon et al., 2009).

To study selectivity for dark targets, we drifted 1.25° × 1.25° targets of varying luminance relative to the background at 45°/s horizontally through the strongest region of the receptive field. Nominal Weber contrasts were calculated from RGB values (linearized monitor, white background 315 $Cdm^{-2}$), C = (target − background)/background.

To test the sensitivity to single contrast edges versus discrete targets, we presented different combinations of stimuli comprising "OFF" and "ON" edges, as well as "Target" features (see Fig. 2). Each stimulus had identical, limited spatial extent (1.25°) in the axis orthogonal to its motion. These were each presented at four different locations within CSTMD1's ~80° wide receptive field (at 5° separations), with a minimum 50 s interval between stimuli presented at the same receptive field location, thus minimizing local habituation effects. Edges and targets were presented at high contrast (see Fig. 2*A*), low contrast (see Fig. 2*B*), and at both contrast polarities (see Fig. 2*C*).

*ESTMD model.* We implemented a model for an ESTMD in MATLAB as described in detail previously (Wiederman et al., 2008, 2009, 2010). This model accounts for the size and velocity tuning observed in insect STMDs and is robust in the presence of background clutter, even without relative motion cues (Wiederman et al., 2008), as observed in physiological responses of STMDs (Nordström and O'Carroll, 2006; Wiederman and O'Carroll, 2011). Parameters are based on fly physiology, with modification to match velocity tuning of the dragonfly (Geurten et al., 2007). Briefly, 2D spatial input is optically blurred (FWHM 1.4°) and hexagonally sampled (1° interreceptor angle) at each time step (1 KHz). Photoreceptor dynamics are based on the model proposed by van Hateren and Snippe (2001). Spatial antagonism of the first-order interneurons (LMCs) was implemented via weighted subtraction of nearest neighbors in the hexagonally sampled inputs to allow transmission of 70% static luminance and thus match the weak lateral inhibition described from LMC recordings in the same dragonfly species (Laughlin, 1974). LMC temporal filters were derived from Juusola et al. (1995), implemented with a relaxed high-pass filter (lower corner frequency 8 Hz) and a small DC component (10%).

The LMC output was fed into an additional stage that took inspiration from electrophysiological recordings from rectifying transient cells (RTCs) described from the locust medulla (Osorio, 1991, O'Carroll et al., 1992), and first optic chiasm and the medulla of the blowfly (Jansonius and van Hateren, 1991; Wiederman et al., 2008). In these RTCs, transient ON and OFF phases (from the LMC high-pass filtering) are separated via a further temporal high-pass filter ($\tau = 100$ or 200 ms) to remove any sustained signal component before half-wave rectification with each channel exhibiting independent and fast adaptation. Adaptation states for this stage are determined by a nonlinear filter that approximates cellular "fast depolarization and slow repolarization" responses, which switches its time constant dependent on whether the input is increasing or decreasing ("fast," $\tau = 3$ ms, when channel input is increasing; and "slow," $\tau = 70$ ms, when decreasing). A key property that results from inclusion of this complex, nonlinear filtering is the selectivity for "novel" transient contrast changes, with the suppression of fluctuating textural variations. This temporal processing thus explains the robustness of STMD neurons to contrasting targets against complex backgrounds.

The next model stage includes strong surround antagonism with ON channels inhibiting ON and OFF inhibiting OFF, as clearly observed in blowfly RTCs (Jansonius and van Hateren, 1993). This "like" channel inhibition is essential to suppress responses for features that are extended along the axis orthogonal to their motion (i.e., the "hypercomplex property" selectivity for small objects vs extended bar features) (Nordström and O'Carroll, 2009). The RTC output then combines ON and OFF channels via a facilitatory interaction between the delayed OFF channel (low-pass filter, $\tau = 25$ ms) and the undelayed ON channel. This is modeled with a multiplication operation; for generality, linear terms may also be included as follows: $a \cdot [\mathrm{ON}] + b \cdot [\mathrm{OFF}_{\mathrm{delayed}}] + c \cdot [\mathrm{ON}] \cdot [\mathrm{OFF}_{\mathrm{delayed}}]$.

*Comparison of ESTMD and EMD models.* For comparison with the ESTMD, EMD models were implemented using the basic schemes described for a 2-detector EMD by Eichner et al. (2011) and a 6-detector EMD by Clark et al. (2011), except that these were implemented using the same optical blur, hexagonal sampling, interreceptor angle, and early visual filtering as the ESTMD described above (i.e., photoreceptor and LMC stages). The signal was then half-wave rectified into ON and OFF channels. The 2-detector EMD model sums the output of individual correlations between ON with ON ("L1 pathway," see Fig. 1*B*) and OFF with OFF ("L2 pathway") channels. The 6-detector model (see Fig. 1*C*) includes additional correlations between opposite signs of contrast polarity (weighted as in Clark et al., 2011) (i.e., correlations between ON with OFF channels as well as between OFF with ON channels).

Both EMD and ESTMD models were implemented as a hexagonal grid of local detectors spanning an 80° × 80° field. Data in Figure 6 were from a single ESTMD within this grid, centered on the target trajectory. Data in Figure 7 were summed over the entire array to mimic the output of a higher-order lobula plate tangential neuron and allow us to measure responses where the leading and trailing edges of the bar stimuli may be widely separated.

## Results

### ESTMD model

Although variants of the HR model (Fig. 1*A*) have previously been used to model spatiotemporal tuning of STMD neurons (Geurten et al., 2007; Dunbier et al., 2011, 2012), these models lack the size selectivity that characterizes STMDs. We therefore previously proposed the ESTMD (Fig. 1*D*) as a model for a fundamental, local signal processing stage underlying STMD behavior (Wiederman et al., 2008, 2009), which is then summed spatially by wider-field STMD neurons amenable to electrophysiological study.

Like the 2-detector EMD proposed by Eichner et al. (2011) (Fig. 1*B*), our ESTMD model incorporates separation of half-wave rectified ON and OFF channels. In *Drosophila*, behavioral responses provide evidence for additional OFF-ON and ON-OFF interactions (Fig. 1*C*) that characterize a more complex 6-detector EMD model (Clark et al., 2011). Unlike the 2-detector EMD, but as in two subunits of the 6-detector model, the ESTMD involves correlation of opposite sign channels (Fig. 1*D*). Unlike any variant of the EMD proposed to date, however, the ESTMD correlates ON with delayed OFF signals arising at the same retinotopic location, rather than from adjacent or nearby detector pairs. This exploits properties of a spatially circumscribed feature moving in a given direction: even against cluttered backgrounds, such a feature is likely to have a leading edge luminance change opposite in sign to its trailing edge. A tiny dark object crossing the receptive field of a single photoreceptor would thus produce a response that first falls before rising.

The addition of strong surround antagonism within the ESTMD further enhances small target selectivity along the axis orthogonal to its motion, whereas rapid adaptation in the rectifying ON/OFF elements rejects repetitive local flicker stimuli induced by background texture. Although STMD neurons show varying degrees of direction selectivity (O'Carroll, 1993; Nordström and O'Carroll, 2006; Barnett et al., 2007), the ESTMD model as originally formulated (Wiederman et al., 2008) is inher-

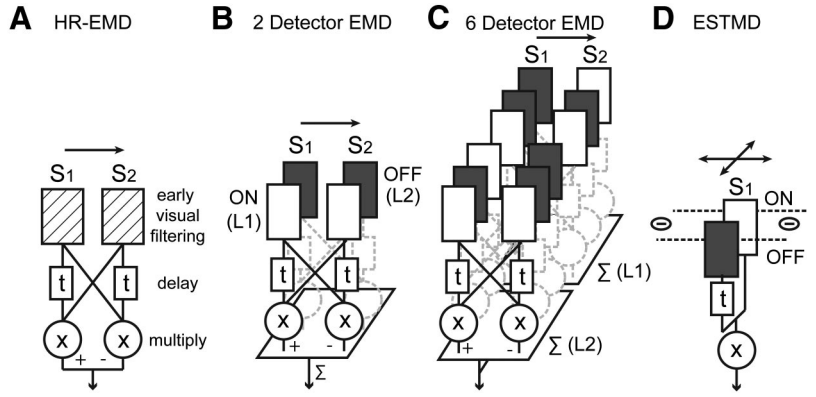


**Figure 1.** Correlation-based models of elementary motion detection. ***A***, The HR-EMD correlates spatially separated luminance signals ($S_1$ and $S_2$) with one path delayed in time. The subtraction of a mirror symmetric unit provides opponent direction selectivity to the EMD. ***B***, In the 2-detector EMD (Eichner et al., 2011), like channels are correlated with one another: ON with ON (L1) and OFF with OFF (L2). L1 and L2 refer to types of laminar monopolar cell. ***C***, The 6-detector EMD (Clark et al., 2011) has more complex combinatorial interactions between channels, including correlation between spatially separated OFF and ON signals. ***D***, In the ESTMD model, center-surround antagonism of ON and OFF channels is followed by the correlation of the delayed OFF with the undelayed ON signal.

ently nondirectional. The inclusion of direction selectivity in the ESTMD, however, can be readily modeled by several alternative mechanisms without changing the fundamental selectivity for small features (Wiederman and O'Carroll, 2013a). These include spatial separation of the correlated ON and OFF channels, asymmetry in the inhibitory surround, or second-order ESTMD-like correlation of inputs derived from 2-detector EMDs (or vice versa).

### Selectivity for dark features

An untested prediction arising from the opposite-polarity correlation in the ESTMD model is its selectivity for the sign of the contrast "signature" produced by a given target. The detection of both light and dark targets would require local ESTMD pairs to correlate both delayed ON with OFF, and delayed OFF with ON channels, whereas a simpler ESTMD (as in Fig. 1*D*) would be selective for dark features. To test whether this is the case, we quantified contrast sensitivity of 10 feature-detecting neurons by drifting small light (i.e., an ON-OFF stimulus) or dark (OFF-ON) targets through the receptive field (Fig. 2*A*,*B*).

In six recordings from the identified neuron, CSTMD1 (Fig. 3*A*) and four from unidentified STMDs (Fig. 3*B*), we observed profound dark target selectivity. Figure 3*A* shows mean spike rate for an example CSTMD1 neuron (within a 500 ms analysis window centered on the receptive field) in response to a range of target contrasts of both light and dark polarities (mean ± SEM of 5 trials). As targets get darker, spike rate increases. However, responses to light targets elicit minimal response even at the highest contrast. Data averaged across 5 CSTMD1 neurons (Fig. 3*A*, inset) confirmed selectivity for the polarity of the stimulus, with a significantly larger response to dark ($C_{Weber} = -1$) versus light ($C_{Weber} = 1$) targets ($p = 0.009$, paired $t$ test). Indeed, responses to light targets are not significantly above spontaneous levels.

The four unidentified feature-selective neurons (Fig. 3*B*) all show varying degrees of size selectivity for targets or short bars (determined from size-tuning; Fig. 3*B*, inset) between 1 and 10° (i.e., orthogonal to the direction of travel). In all of these feature-selective neurons, darker targets evoked robust responses saturating at relatively low contrasts ($C_{Weber}$ between −0.2 and −0.5). They all elicit very weak responses to high contrast light targets (Fig. 3*B*), thus confirming that dark target selectivity is not unique to CSTMD1. If we present light targets against a black screen background (a stimulus that represents a much higher Weber contrast), we do see intermittent weak responses (data not shown). We excluded these data from our quantitative analysis, however, because it subjects the photoreceptors to a significantly lower adapting luminance, well below the physiologically normal range.

### Supralinear summation of edges

From Figure 3, we conclude that STMD neurons show dark target selectivity consistent with predictions of an ESTMD model that correlates delayed OFF with ON information. To further test whether this involves a supralinear interaction between these channels, we presented STMD neurons with moving ON and OFF features with limited extent in the dimension orthogonal to their motion (i.e., local edge features) and compared responses with those for the equivalent discrete targets. These stimuli are illustrated by the pictograms in Figures 2 and 4. Figure 4*A* shows mean peristimulus time histograms from two individual CSTMD1s in response to the different stimuli. In the first example, we repeated each stimulus 5 times at 4 locations within the receptive field (20 trials). Both OFF edge (dashed line) and ON edge (dotted line) responses are weak. Target responses (solid line) are greater than the linear combination of the ON and OFF edge responses. In a second CSTMD1 example (16 trials), OFF edges produce moderate responses that are stronger than ON edge responses. Figure 4*B* shows responses to the same stimuli in one of the unidentified neurons (STMD-U1), which also resulted in a supralinear target response. To examine reproducibility of responses in CSTMD1, we pooled results from five neurons (Fig. 4*C*, 1s analysis window, 68 trials). There is a significant difference between all four conditions: ON versus OFF $p < 0.05$, others $p < 0.001$ (Dunn's multiple comparison, Kruskal-Wallis). Furthermore, target responses are significantly higher than the sum of the ON and OFF edge responses ($p = 0.001$, Mann–Whitney U), thus supporting a supralinear interaction between the OFF and ON channels.

With the high contrast stimuli in Figure 4*A*–*C*, many individual trials produce strong edge responses, particularly to the OFF stimulus, and target responses may easily exceed 300 spike/s. Saturation could potentially mask the full degree of the nonlinear interaction between OFF and ON channels. We therefore also presented lower contrast versions of the stimuli (Fig. 2*B*) to two CSTMD1 neurons (16 trials total). This allowed us to also test a further variant, a "double" OFF-edge stimulus, composed of a white to gray followed by a gray to black transition, separated by 1.25° (Fig. 2*B*). This feature induces luminance changes similar in contrast and spatial extent to the low contrast dark target, except that the polarity of the trailing edge is the same as the leading edge. Figure 4*D* shows mean responses to these stimuli in an example CSTMD1, revealing potent supralinearity of the target response relative to ON and OFF edge responses. When pooled over the entire set of 16 trials (Fig. 4*E*), the mean target responses are much larger than for any of the other conditions, including the double OFF-edge stimulus. This suggests that the target response requires both ON and OFF channels.

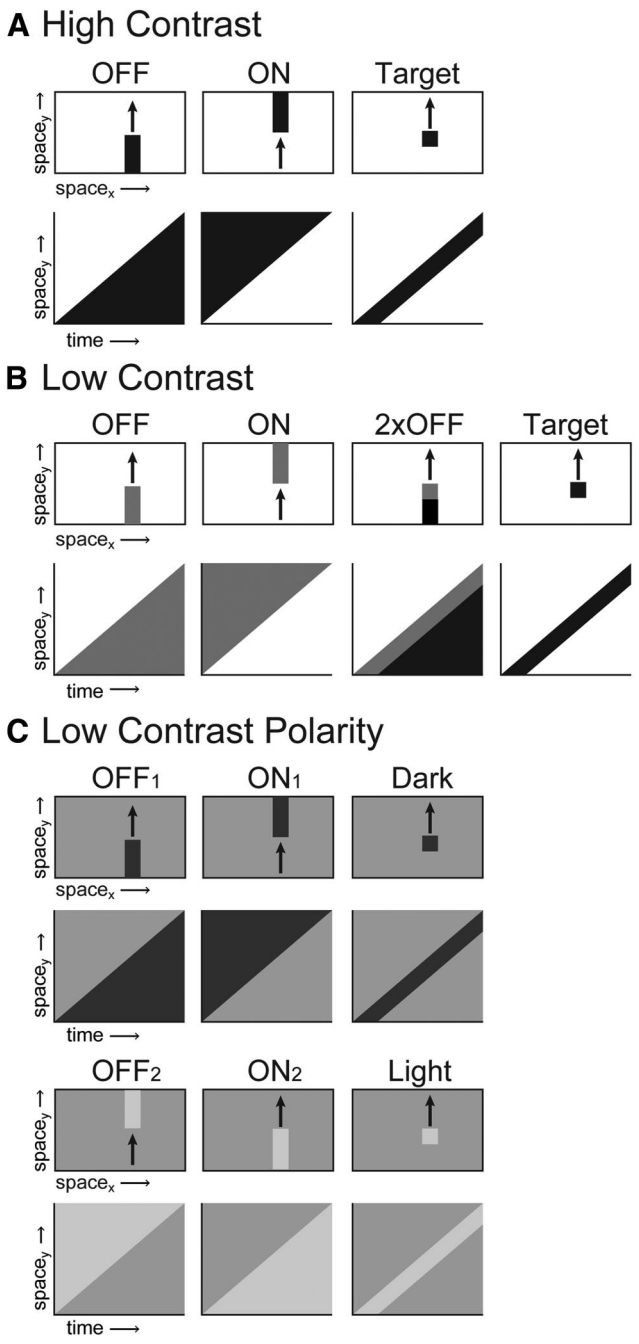


**Figure 2.** Visual stimuli presented to the dragonfly during electrophysiological recordings from STMD neurons. Upper rows of each combination depict a snapshot in time of the 2 d display on which stimuli were presented (not to scale), whereas lower rows are space-time plots for the luminance change along the line that the feature moves. ***A***, High contrast OFF and ON edges and a single black target are drifted from the bottom to the top of the display. ***B***, Low contrast versions of both edges and target, with the addition of a "target" composed of two OFF edges. ***C***, On a mean background, ON and OFF edges are composed from both mean background to light and mean background to dark transitions. Both light and dark targets are also presented.

To test stimuli for both light and dark contrast edge polarities, we also presented low contrast stimuli against a mean luminance (gray) background (Fig. 2*C*) in two further CSTMD1 neurons (Fig. 5*A*, 12 trials). Dark target selectivity is again evidenced by the much stronger response to dark targets than any other combination of light or dark contrasting edges. Some of the variation evident in the box-plot distributions in Figure 5*A* is the result of the inhomogeneous sensitivity at

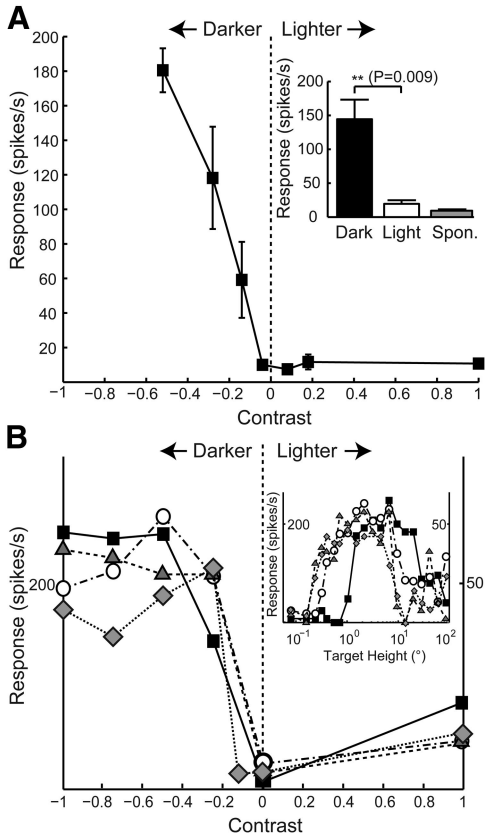


**Figure 3.** Dark target selectivity in the dragonfly brain. ***A***, An individual example of CSTMD1 responses to targets of varying contrast moving on a mid-luminance background (mean ± SEM, 5 trials). Responses strengthen as negative contrast polarity of the target increases (dark); however, positive contrast (light) targets elicit little response. Across 5 neurons (inset graph, mean ± SEM), CSTMD1 displays dark target selectivity, responding significantly more ($p = 0.009$) to high contrast black targets ($C_{Weber} = -1$) than to high contrast white targets ($C_{Weber} = 1$), which are indistinguishable from spontaneous activity. ***B***, Four unidentified neurons in *H. tau* produce robust responses to targets of increasing dark contrast but not to light contrast (left ordinate: black squares and gray diamonds; right ordinate: gray triangles and white circles). These unidentified feature-selective neurons exhibit varying size selectivity (inset graph).

different locations within the receptive field over which stimuli were presented. Figure 5*B* shows individual responses to low contrast dark targets plotted against the sum of the OFF and ON edge responses matched to the same location in the receptive field. Observed responses to low contrast dark targets are clearly always much stronger (dashed line, slope = 1.9 ± 0.4 [95% CI]) than the predictions of the linear sum of ON and OFF responses (solid line, slope = 1).

### Evidence for an ESTMD-like mechanism

Together, our experimental data confirm the following: (1) only dark targets evoke robust spiking activity from CSTMD1; (2) the target response involves a potent supralinear interaction between nearby edges; and (3) the target response requires both OFF and ON components. Can we reproduce these results with the ESTMD model that we previously proposed (Wiederman et al., 2008)? Figure 6 shows data for ESTMD models that include ON and OFF channels that interact both linearly and multiplicatively: $a \cdot [\mathrm{ON}] + b \cdot [\mathrm{OFF}_{\mathrm{delayed}}] + c \cdot [\mathrm{ON}] \cdot [\mathrm{OFF}_{\mathrm{delayed}}]$. The data show distributions for outputs of our model in response to similar stimuli to those presented to STMD neurons in Figures 4 and 5 (i.e., at both high and low contrast) and using combinations of coefficients *a*, *b*, and *c* varied over a large range as follows: *a* {0, 1, 2};

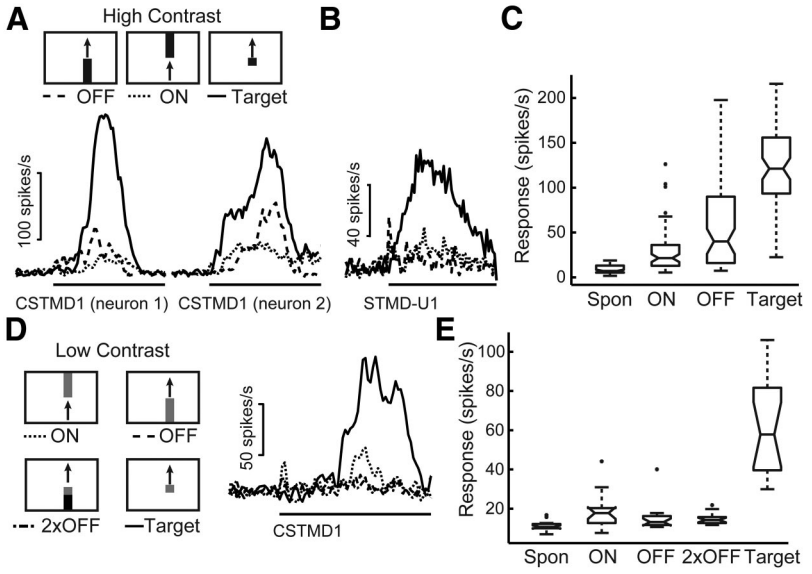


**Figure 4.** Target responses are more than the linear combination of responses to ON and OFF edges. ***A***, Two examples of individual CSTMD1 responses to high contrast stimuli drifted through the receptive field. In the first example, CSTMD1 exhibits little response to either ON or OFF edges, and the response to targets is larger than a linear combination of the edge responses (mean of 20 trials). In the second example, CSTMD1 responds to high contrast ON and OFF edges, although both are weaker than target responses (mean of 16 trials). ***B***, The response of an unidentified STMD neuron to the same stimuli exhibits a similar supralinearity (mean of 20 trials). ***C***, Pooled CSTMD1 responses (68 trials >5 neurons) show that median target responses are larger than the linear combination of responses to ON and OFF edges (Target vs ON + OFF, $p = 0.001$, Mann–Whitney U). In some trials, edge responses evoke responses from CSTMD1, in particular to the OFF stimulus. ***D***, CSTMD1 responses to lower contrast target and edge stimuli ($C_{Weber} = -0.6$) and a "double" OFF edge stimulus (white to gray to black). An example CSTMD1 response to the lower contrast stimuli exhibits strong target responses and weak response to either ON or OFF edges. Furthermore, the double OFF/OFF stimulus elicits minimal response (average of 12). ***E***, CSTMD1 target responses are greater than any linear combination of the ON and OFF edge responses (16 trials >2 neurons).

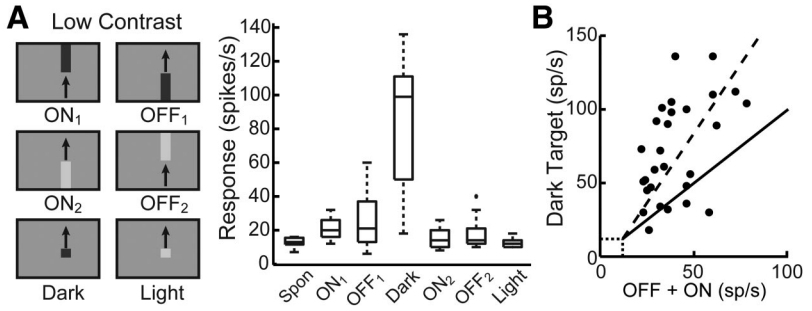


**Figure 5.** CSTMD1 responses to low contrast edge and target stimuli ***A***, Regardless of the edge transition with respect to the background (i.e., $ON_1$, dark to mean; or $ON_2$, mean to light; $OFF_1$, mean to dark; or $OFF_2$, light to mean), CSTMD1 responses in a further two neurons (12 trials total) are much stronger to the dark target. These dark target responses are much larger than those to the light target or the linear combination of either of the ON and OFF edge combinations. ***B***, CSTMD1 responses to low contrast dark targets are plotted against the linear sum of ON and OFF responses (matched at the same receptive field location). Solid line indicates a linear combination (slope of 1); dashed line indicates best fit (slope = 1.9 ± 0.4 [95% CI]).

$b$ {0, 1, 2}; and $c$ {1, 2, 5}. These combinations of term coefficients allow us to represent different "balances" of interactions between separate ON and OFF channels.

As can be seen from Figure 6, the ESTMD model captures not only the supralinear interaction between the ON and OFF components of the target stimulus, it also predicts the presence of weak responses to the ON and particularly the OFF edges at high contrasts (Fig. 6*A*,*B*), as we observed in the STMD recordings (Figs. 4 and 5). This is perhaps surprising given that the distributions include combinations of term coefficients where $a = b = 0$ (i.e., a purely multiplicative ESTMD). However, with appropriate temporal high-pass filtering in early vision, a single-edge stimulus can potentially induce excitation of both ON and OFF channels because of response rebound after the initial luminance change. Even in the photoreceptors themselves, luminance step responses may show complex multiphasic transients at high contrasts, even though they encode luminance steps faithfully at low contrasts (Laughlin and Weckström, 1993). Such complex temporal filtering would lead to weak outputs from even a purely multiplicative ESTMD. In addition to varying the term coefficients, we further tested two model variants ($\tau = 200$ ms, $\tau = 100$ ms) that simulate variation in high-pass filtering that could represent differences in the state of light adaptation (Juusola et al., 1995; van Hateren and Snippe, 2001) or even a change in temperature (Tatler et al., 2000). At low contrasts (Fig. 6*C*,*D*), the model is relatively robust against the differing contributions of the term coefficients within the range we considered, and always shows the strongly supralinear interaction effect as seen in the physiological data (Figs. 4 and 5). The faster time constant model better matches the physiological data, however, in that it gives stronger responses to dark edges at high but not lower contrast (compare Fig. 6*B*,*D* with Fig. 4*C*,*E*).

### Comparison with EMD models

From Figure 6, we conclude that, with careful attention to the temporal properties of high-pass filters that are a key element of the model, an ESTMD-like mechanism can explain selectivity for dark features and the supralinear interaction between nearby ON and OFF edges that we observe in STMD neurons. Could a simple HR correlation EMD be an alternative explanation for our data? The HR-EMD also includes a multiplicative interaction, and it is entirely possible that subsequent spatial processing, such as lateral inhibition, could support small-object tuning based on EMD outputs. Furthermore, the varying degrees of directional sensitivity observed in STMD neurons (Barnett et al., 2007) might be explained by combinations of signals derived from EMDs with different spatial alignments.

On the contrary, however, corresponding models for both a 2- and 6-detector EMD yield sublinear addition of the single-edge responses compared with the response to the tiny targets used in our experiments (Fig. 7*A*,*B*). This is in contrast to the output supralinearity observed in our ESTMD model (Fig. 7*C*). This is because optical blur by the facet lenses (Horridge, 1978; Nordström and O'Carroll, 2006) has a greater effect on the small targets compared with the single-edge stimuli, which are blurred only across their narrow dimension. Therefore, compared with

the moving edges, target responses are expected to be weaker at the earliest stages of visual processing, despite a front end for all three model variants that accounts well for both linear and nonlinear spatiotemporal filtering in early visual processing (Laughlin, 1974; van Hateren and Snippe, 2001; Brinkworth et al., 2008; Mah et al., 2008; Wiederman et al., 2010). This makes the observed strength of the response to the target versus single edges in the STMD recordings all the more impressive.

Arguably, the contrast attenuation of small features could be partially offset by the strong surround antagonism that represents an additional stage of the ESTMD model. We tested this by simulation of additional variants of the 2- and 6-detector EMD models that include this extra stage of processing (Fig. 7*B*). Again, target responses are weaker than the linear combination of the single-edge responses. If we extend the target width in the direction of travel (Fig. 7*D*), optical blur has less effect on the target, which begins to resemble a double-edge stimulus (i.e., an OFF leading edge widely separated from an ON trailing edge). With two-edge features within the scene, both EMD variants tested then yield responses greater than ON or OFF edge stimuli alone but never exceed the linear combination of ON and OFF edge responses (Fig. 7*D*). The ESTMD, by comparison, responds progressively more weakly (as observed in STMD neurons) as the leading and trailing edge become further separated in time.

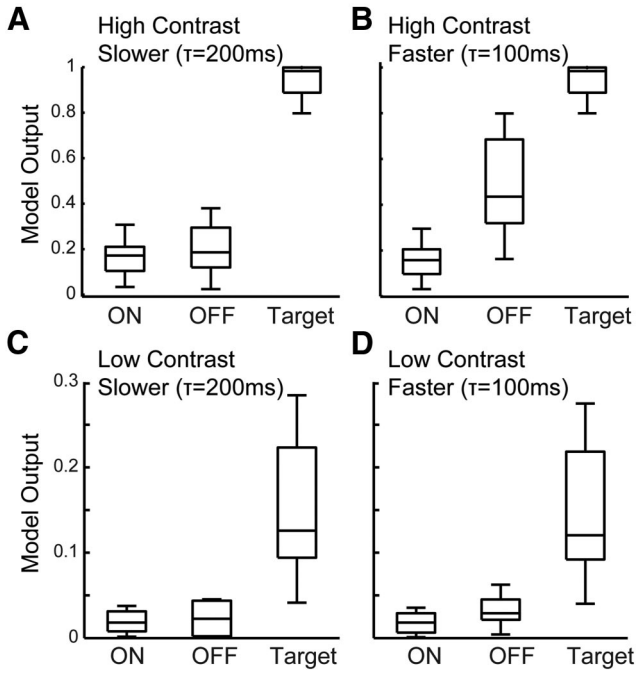


**Figure 6.** An ESTMD model includes terms for separate ON and OFF channels, as well as a facilitatory correlation between the delayed OFF and undelayed ON signals. $a \cdot [\mathrm{ON}] + b \cdot [\mathrm{OFF}_{\mathrm{delayed}}] + c \cdot [\mathrm{ON}] \cdot [\mathrm{OFF}_{\mathrm{delayed}}]$. We varied $a$–$c$ coefficients and examine their pooled effect on each distribution of ON edge, OFF edge, and target responses. All model variants predict supralinear target responses, ***A***, High contrast stimuli and more sustaining high-pass filtering ($\tau = 200$ ms) predict either or both ON and OFF edge responses. ***B***, High contrast and more transient high-pass filtering ($\tau = 100$ ms) produces larger OFF edge responses, as observed in experiments (compare ***B*** with Fig. 4*C*). ***C***, For lower contrast stimuli, the ESTMD model predicts minimal ON or OFF edge responses, again matching the physiological data (compare ***C***,***D*** with Figs. 4*E* and 5*A*).

## Discussion

STMDs are tuned to the velocity of a moving target, itself indicative of an underlying correlation mechanism (Nordström and O'Carroll, 2006; Geurten et al., 2007). Although we previously suggested this provides evidence for an HR-EMD framework, the result is also consistent with an ESTMD correlation model. There is a pronounced velocity optimum that would be determined by early visual filtering and the correlation delay time constant (Geurten et al., 2007; Dunbier et al., 2012), with the optimum velocity increasing as target width increases in the direction of travel (Geurten et al., 2007). This is the result of the increased spatial separation between the leading and trailing edge of the target, requiring a faster transit speed to match a given delay between OFF and ON channels. The ESTMD, as a "temporal" correlator, can extract this weak rising and falling signature of a target even though it primarily occurs in a single ommatidium at a time. Although directionality may be readily explained with the inclusion of spatial interactions or asymmetry (Wiederman and O'Carroll, 2013a), a benefit of (purely local) temporal processing is the robust responses to slowly moving targets smaller than a single ommatidium, a simple form of hyperacuity. Indeed, many STMD neurons (including CSTMD1) are responsive to target sizes of <0.5° square, which are of extremely low effective contrast (*Eristalis tenax*, Nordström and O'Carroll, 2006; *H. tau*, Wiederman and O'Carroll, 2013b).

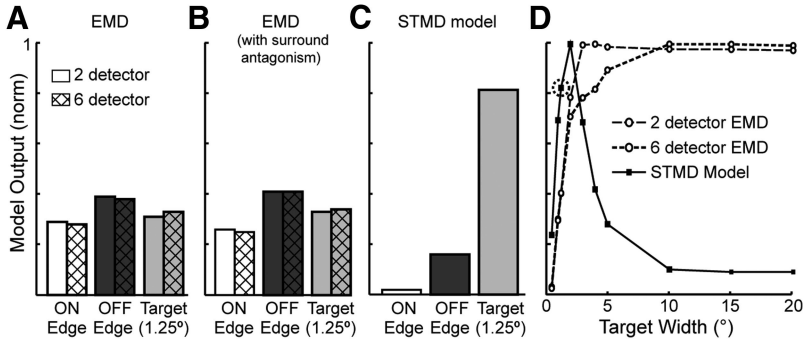


**Figure 7.** Edges (ON and OFF) and dark targets serve as input to model variants of the EMD as well as the ESTMD model. These include both the 2-detector EMD, which sums channels of 'like" correlations (Eichner et al., 2011) and the 6-detector EMD, which includes terms between ON and OFF correlations (Clark et al., 2011). Each of these versions is modeled with and without strong surround antagonism. For each model variant, output is normalized to the sum of the OFF edge, ON edge, and target output values. ***A***, Without surround antagonism, both the 2- and 6-detector models predict a sublinear response to targets rather than the supralinearity observed in CSTMD1 (Figs. 4*C*,*E* and 5). ***B***, Model outputs do not change when surround antagonism is included in the model variants. ***C***, In comparison, an STMD model matches the physiological data with target responses much larger than the linear combination of ON and OFF edge responses. ***D***, EMD and STMD model output in response to targets of varying extent (in the direction of travel). The ESTMD model is more responsive to small targets, and the output of the OFF and ON correlation is inherently tuned to the separation of the OFF and ON edges in the direction of travel (i.e., velocity/width tuned).

Our modeling shows that the pattern of responses observed in STMD neurons to single-edge versus target features is poorly predicted by HR-EMDs but well predicted by an ESTMD mechanism. A side effect of the very high gain required to achieve the observed sensitivity for the blurred image of very small targets is some sensitivity to high contrast edges with limited angular extent. Natural scenes, however, are dominated by larger features (Dror et al., 2000), and our own recording from STMDs in response to natural scenes shows that breakthrough responses from textural features of the background are weak even in strong clut-

ter (Wiederman and O'Carroll, 2011). To account for some ON and OFF edge excitation, we include linear terms in our phenomenological model. What would the three terms of our model represent physiologically? They suggest a mechanism of interaction that involves weak excitation by the individual signals that impinge on the individual arms of the correlator, with significant enhancement of excitation by their coactivation. Significant variation in single-edge sensitivity seen in CSTMD1 from animal to animal could reflect varying excitation thresholds or variation in the strengths of the individual inputs relative to their degree of mutual facilitation.

Hawking dragonflies, such as *H. tau*, remain continuously in flight, swooping upward to catch their prey overhead (Corbet, 1999). In this scenario, the target prey is located within an area of high visual acuity (Horridge, 1978) and will appear dark against a light sky background. However, we also observe dragonflies chasing prey and conspecifics against cluttered surrounds, with the changing background causing the perceived target to alternate between light and dark contrasts. From the behavioral perspective, it would seem that neurons responsive to either or both light and dark targets should exist. Our encountering of only dark target selective neurons to date may be coincidental or possibly the result of bias in our experimental preparation, which is geared toward recording neurons with dorsally centered receptive fields. From the modeling perspective, should light-target selectivity be observed in future, this problem is readily solved with the inclusion of an $[ON_{delayed}] \cdot [OFF]$ term to form a light-target-sensitive ESTMD.

Although we present results from several types of STMD neurons, our primary evidence is derived from recordings of CSTMD1. This neuron has visual inputs in the midbrain and has recently been shown to exhibit several "higher-order" attributes. These include the ability to selectively attend to a single target in the presence of a distractor (Wiederman and O'Carroll, 2013b), as well as exhibiting a slow facilitation of its response for targets that move along a continuous trajectory (Nordström at al. 2011; Dunbier et al., 2012). However, CSTMD1 is a neuron that responds very quickly in absolute terms, with a response latency $<$50 ms (Nordström et al., 2011) and tuning to high target velocity (Geurten et al., 2007; Dunbier et al., 2012). Our modeling of its response kinetics suggests that the facilitation must be the result of a higher-order property within the STMD pathway (e.g., attentional modulation) in response to slower moving features, rather than any inherent sluggishness in the time constants of the underlying motion pathway (Dunbier et al., 2011, 2012). Thus, some caution is still in order in attributing the observed supralinear response characteristics of CSTMD1 to an underlying elementary correlation between local OFF and ON channels, versus a mechanism that upregulates attention for the highly salient target stimulus. Nevertheless, the fact that we also observed similar supralinearity in several other unidentified STMD neurons suggests that this is a common property of the input pathway.

## References


Barnett PD, Nordström K, O'Carroll DC (2007) Retinotopic organization of small-field-target-detecting neurons in the insect visual system. Curr Biol 17:569–578. CrossRef Medline

Bolzon DM, Nordström K, O'Carroll DC (2009) Local and large-range inhibition in feature detection. J Neurosci 29:14143–14150. CrossRef Medline

Borst A, Euler T (2011) Seeing things in motion: models, circuits, and mechanisms. Neuron 71:974–994. CrossRef Medline

Brinkworth RSA, Mah EL, Gray JP, O'Carroll DC (2008) Photoreceptor processing improves salience facilitating small target detection in cluttered scenes. J Vis 8(11):1–17. CrossRef Medline

Clark DA, Bursztyn L, Horowitz MA, Schnitzer MJ, Clandinin TR (2011) Defining the computational structure of the motion detector in Drosophila. Neuron 70:1165–1177. CrossRef Medline

Corbet PS (1999) Dragonflies: behavior and ecology of Odonata. Ithaca: Cornell UP.

Dror R, O'Carroll DC, Laughlin SB (2000) The role of natural images statistics in biological motion estimation. Lect Notes Comput Sci 1811:492–501. CrossRef

Dunbier JR, Wiederman SD, Shoemaker PA, O'Carroll DC (2011) Modelling the temporal response properties of an insect small target motion detector. Proceedings of the 7th International Conference on Intelligent Sensors, Sensor Networks and Information Processing. 125–130.

Dunbier JR, Wiederman SD, Shoemaker PA, O'Carroll DC (2012) Facilitation of dragonfly target-detecting neurons by slow moving features on continuous paths. Front Neural Circuits 6:79. Medline

Egelhaaf M, Borst A (1985) Are there separate ON and OFF channels in fly motion vision? Vis Neurosci 8:151–164. Medline

Eichner H, Joesch M, Schnell B, Reiff DF, Borst A (2011) Internal structure of the fly elementary motion detector. Neuron 70:1155–1164. CrossRef Medline

Franceschini N, Riehle A, Nestour A (1989) Directionally selective motion detection by insect neurons. In: Facets of vision (Stavenga D, Hardie R, eds). New York: Springer.

Geurten BR, Nordström K, Sprayberry JD, Bolzon DM, O'Carroll DC (2007) Neural mechanisms underlying target detection in a dragonfly centrifugal neuron. J Exp Biol 210:3277–3284. CrossRef Medline

Hartline HK (1938) The response of single nerve fibers of the vertebrate eye to illumination of the retina. Am J Physiol 121:400–415.

Hassenstein B, Reichardt W (1956) Analyse der zeit-, reihenfolgen-und vorzeichenauswertung bei der bewegungsperzeption des rüsselkäfers Chlorophanus. Z Naturf 11b:513–524.

Horridge GA (1978) The separation of visual axes in apposition compound eyes. Philos Trans R Soc Lond B Biol Sci 285:1–59. CrossRef Medline

Jansonius N, van Hateren J (1991) Fast temporal adaptation of on-off units in the first optic chiasm of the blowfly. J Comp Physiol A 168: 631–637. Medline

Jansonius NM, van Hateren JH (1993) On-off units in the first optic chiasm of the blowfly: II. Spatial properties. J Comp Physiol A 172:467–471. CrossRef

Joesch M, Schnell B, Raghu SV, Reiff DF, Borst A (2010) ON and OFF pathways in Drosophila motion vision. Nature 468:300–304. CrossRef Medline

Joesch M, Weber F, Eichner H, Borst A (2013) Functional specializations of parallel motion detection circuits in the fly. J Neurosci 33:902–905. CrossRef Medline

Juusola M, Uusitalo RO, Weckström M (1995) Transfer of graded potentials at the photoreceptor-interneuron synapse. J Gen Physiol 105:117–148. CrossRef Medline

Laughlin SB (1974) Neural integration in the first optic neuropile of dragonflies. J Comp Physiol A 92:357–375. CrossRef

Laughlin SB, Weckstrom M (1993) Fast and slow photoreceptors: a comparative study of the functional diversity of coding and conductances in the Diptera. J Comp Physiol A 172:593–609. CrossRef

Mah EL, Brinkworth RS, O'Carroll DC (2008) Implementation of an elaborated neuromorphic model of a biological photoreceptor. Biol Cybern 98:357–369. CrossRef Medline

Nordström K, O'Carroll DC (2006) Small object detection neurons in female hoverflies. Proc R Soc B 273:1211–1216. CrossRef Medline

Nordström K, O'Carroll DC (2009) Feature detection and the hypercomplex property in insects. Trends Neurosci 32:383–391. CrossRef Medline

Nordström K, Bolzon DM, O'Carroll DC (2011) Spatial facilitation by a high-performance dragonfly target-detecting neuron. Biol Lett 7:588–592. CrossRef Medline

Nordström K, Barnett PD, O Carroll DC (2006) Insect detection of small targets moving in visual clutter. PLoS Biol 4:378–386.

O'Carroll D (1993) Feature-detecting neurons in dragonflies. Nature 362: 541–543. CrossRef

O'Carroll DC, Osorio D, James AC, Bush T (1992) Local feedback mediated via amacrine cells in the insect optic lobe. J Comp Physiol A 171:447–455.

O'Shea M, Williams JLD (1974) The anatomy and output connection of a

locust visual interneurone: the lobular giant movement detector (LGMD) neurone. J Comp Physiol A 91:257–266. CrossRef

Osorio D (1991) Mechanisms of early visual processing in the medulla of the locust optic lobe: how self-inhibition, spatial-pooling, and signal rectification contribute to the properties of transient cells. Vis Neurosci 7:345–355. CrossRef Medline

Strausfeld NJ (1976) Atlas of an insect brain. New York: Springer.

Tatler B, O'Carroll DC, Laughlin SB (2000) Temperature and the resolving power of fly photoreceptors. J Comp Physiol A 186:399–407. CrossRef

van Hateren JH, Snippe HP (2001) Information theoretical evaluation of parametric models of gain control in blowfly photoreceptor cells. Vision Res 41:1851–1865. CrossRef Medline

Wiederman SD, O'Carroll DC (2011) Discrimination of features in natural scenes by a dragonfly neuron. J Neurosci 31:7141–7144. CrossRef Medline

Wiederman SD, O'Carroll DC (2013a) Selective attention in an insect visual neuron. Curr Biol 23:156–161. CrossRef Medline

Wiederman SD, O'Carroll DC (2013b) Biomimetic target detection: modeling 2nd order correlation of OFF and ON channels. Proceedings of the 2013 IEEE Symposium Series on Computational Intelligence for Multimedia, Signal and Vision Processing, Singapore (in press).

Wiederman SD, Brinkworth RSA, O'Carroll DC (2009) Bio-inspired small target discrimination in high dynamic range natural scenes. 3rd International Conference on Bio-Inspired Computing: Theories and Applications 2008. 109–116.

Wiederman SD, Brinkworth RSA, O'Carroll DC (2010) Performance of a bio-inspired model for the robust detection of moving targets in high dynamic range natural scenes. J Comput Theor Nanos 7:911–920. CrossRef

Wiederman SD, Shoemaker PA, O'Carroll DC (2008) A model for the detection of moving targets in visual clutter inspired by insect physiology. PLoS One 3:e2784. CrossRef Medline